Carbohydrate Polymers 206 (2019) 749–756

Contents lists available at ScienceDirect

Carbohydrate Polymers

journal homepage: www.elsevier.com/locate/carbpol

Effects of pH, extrusion tip size and storage protocol on the structural properties of Ca(II)-alginate beads

Ignacio Zazzali[a,b], Tatiana Rocio Aguirre Calvo[a,b], Víctor Manuel Pizones Ruíz-Henestrosa[b], Patricio R. Santagapita[a,b,*], Mercedes Perullini[c,d,**]

[a] Universidad de Buenos Aires. Facultad de Ciencias Exactas y Naturales, Departamentos de Industrias y Química Orgánica, Buenos Aires, Argentina
[b] CONICET-Universidad de Buenos Aires, Instituto de Tecnología de Alimentos y Procesos Químicos (ITAPROQ), Buenos Aires, Argentina
[c] Universidad de Buenos Aires, Facultad de Ciencias Exactas y Naturales, Departamento de Química Inorgánica, Analítica y Química Física, Buenos Aires, Argentina
[d] CONICET-Universidad de Buenos Aires, Instituto de Química Física de los Materiales, Medio Ambiente y Energía (INQUIMAE), Buenos Aires, Argentina

ARTICLE INFO

Keywords:
Encapsulation
SAXS
Microstructure
Alginate
Diffusion coefficient
Water content and activity

ABSTRACT

The Ca(II)-alginate beads were formulated changing some synthesis variables: pH (3.8–6.8), extrusion tip size (0.25–0.50 mm) and washing/storage protocol, to evaluate possible implications in the structural properties of beads, which are critical to scale and standardize their production at industrial level. Regardless of the macro- (diameter, area, perimeter and roundness, studied by image analysis) and micro-structural (size, density and interconnectivity of rods assessed by SAXS) parameters analyzed, there are no effects related to the washing and storage protocol employed for any synthesis conditions. Structural parameters are only influenced by the synthesis pH. Both washing protocol and extrusion tip size effects on the consolidation of the alginate network are negligible at each pH value. Besides, none of the synthesis variables affected the availability of water within the beads as assessed by diffusion coefficient and water activity measurements. A model, relating chain-chain interactions and polymer chain packing, is proposed.

1. Introduction

In recent decades, encapsulation has been widely studied to improve delivery systems in pharmaceutical (Hoare & Kohane, 2008), food-science (Li et al., 2017), medical (Bhujbal, de Vos, & Niclou, 2014), and technological (Biswas, Chattopadhyy, Sen, & Saha, 2015; Sarkar, Sahoo, Das, Prusty, & Swain, 2017) applications by conserving bioactive compounds from environmental conditions (Wandrey, Bartkowiak, & Harding, 2009). The use of low-cost materials that are also bioavailable and biodegradable has led most biopolymer-based encapsulation studies (Wandrey et al., 2009). Currently alginate is a commonly chosen biopolymer used to produce encapsulation matrices due to its ease handling, biodegradability, low-cost, and non-toxicity, and is deemed as 'generally recognized as safe' (GRAS) (Nedovic, Kalusevic, Manojlovic, Levic, & Bugarski, 2011; Rowley, Madlambayan, & Mooney, 1999). Gelation of alginate was widely used for immobilization of bio-entities, from macromolecules to metazoans (Perullini, Orias, Durrieu, Jobbágy, & Bilmes, 2014; Santagapita, Mazzobre, & Buera, 2011).

Alginate is a naturally occurring anionic and hydrophilic linear polymer, derived primarily from brown seaweed and bacteria. Alginate contains blocks of (1–4)-linked β-D-mannuronic acid (M) and α-L-guluronic acid (G) forming regions of M and G blocks as well as alternating MG blocks (Lee & Mooney, 2012). Crosslinking with divalent cations, such as Zn^{2+}, Ca^{2+}, and Ba^{2+}, is regularly employed as a method to prepare alginate hydrogels from an aqueous solution under gentle conditions. Divalent and trivalent cations bind into the cavities of contiguous G blocks of alginate (Stokke et al., 2000) in a highly cooperative manner, thus forming a gel, with a structure commonly known as "egg-box" (He, Liu, Li, & Li, 2016; Narayanan, Melman, Letourneau, Mendelson, & Melman, 2012; Sonego, Santagapita, Perullini, & Jobbágy, 2016).

Additionally, the sodium alginate solution can be gelled at acidic pH, below the pKa value of the uronic acid residues (3.38 and 3.65 for M and G residues, respectively) (Draget & Taylor, 2011), mediated by chain–chain interactions leading to gelation, once a critical fraction of

* Corresponding author at: Universidad de Buenos Aires. Facultad de Ciencias Exactas y Naturales, Departamentos de Industrias y Química Orgánica, Buenos Aires, Argentina.
** Corresponding author at: Universidad de Buenos Aires, Facultad de Ciencias Exactas y Naturales, Departamento de Química Inorgánica, Analítica y Química Física, Buenos Aires, Argentina.
E-mail addresses: prs@di.fcen.uba.ar (P.R. Santagapita), mercedesp@qi.fcen.uba.ar (M. Perullini).

https://doi.org/10.1016/j.carbpol.2018.11.051
Received 11 July 2018; Received in revised form 3 November 2018; Accepted 16 November 2018
Available online 19 November 2018
0144-8617/

carboxylate residues is protonated with a concomitant decrease in the polymer charge density. Control over the velocity of the proton-gelation front allows the formation of a hydrogel shell while the core remains liquid, allowing the encapsulation of pH sensitive bio-entities (Spedalieri et al., 2015). The proton-driven alginate gelation (H–alginate) occurs around pH 3.5, depending on the M/G relative content of the employed alginate. In H-alginate hydrogels, homopolymeric M-blocks create stable bonds to a lesser extent than G-blocks. Therefore, the molecular configuration, as well as the influence of the synthesis conditions is crucial in understanding and maintaining the stability of encapsulated compounds which can present different interactions with the matrix according to their physicochemical properties.

Small angle X-ray scattering (SAXS) is a powerful method which allows the analysis of structural characteristics of the alginate hydrogels. SAXS has been employed to elucidate the structural modifications induced by different crosslinking cations as well as acidic conditions (Agulhon, Robitzer, David, & Quignard, 2012; Stokke et al., 2000), the effect of excipients addition (Traffano-Schiffo, Castro-Giraldez, Fito, Perullini, & Santagapita, 2018), and the incorporation of encapsulated compounds (Aguirre-Calvo, Perullini, & Santagapita, 2018).

To scale and standardize the process of alginate beads production at an industrial level, it is mandatory to assess the production parameters affecting the gel formation and comprehend their implications in the macro and microstructure of the resulting beads. For instance, the amount and activity of water contained within the beads are important parameters to assess, considering the prospect of biotechnological applications. Then many important properties such as water uptake and bead expansion are related to the water content and are of particular interest in biological systems since they modulate the exchange of nutrients and the release of bioactive compounds from these systems (Aguirre Calvo, Busch, & Santagapita, 2017). On the other hand, it has been reported that freshly formed alginate beads should be maintained in the gelling bath for a period, followed by removal of residual Ca^{2+} ions by washing with distilled water, to allow for complete consolidation of the egg box network (Deladino, Anbinder, Navarro, & Martino, 2008). However, it would be of great interest from a time and economic standpoint if this process could be ruled out. Furthermore, since most natural extracts used in the food industry as bioactive compounds sources have acidic pH value, it is of significance to evaluate possible contributions of alginate chain-chain interaction to the gel structure of beads when formed by ionotropic gelation at acidic conditions and near the pKa value. Thus, the aim of this study was to formulate Ca(II)-alginate beads modifying some of the possible synthesis variables, namely, pH, extrusion tip size and washing protocol in order to evaluate possible implications in the structural properties of beads.

2. Materials and methods

2.1. Materials

Sodium alginate: Algogel 5540 (Cargill S.A. San Isidro, Buenos Aires, Argentina), molecular weight of 1.97 (± 0.06) 10^5 g/mol and mannuronate/guluronate ratio of 0.6; $CaCl_2.2H_2O$ (Cicarelli S.A., Argentina). Hydrochloric acid 37% (w/w) (Anedra, Research AG S.A., Tigre, Argentina).

2.2. Beads preparation

Sodium alginate (1.5% w/v) and calcium chloride dihydrate (2.5% w/v) solutions were prepared separately under constant stirring with distilled water until complete dissolution. Both solutions were adjusted to three different pH values (3.8; 5.0 and 6.8) with diluted HCl solution. Beads were prepared by ionotropic gelation according to the dropping method (Aguirre Calvo & Santagapita, 2016). Briefly, 6 mL of the alginate solution were dripped using a peristaltic pump model BT50-1J JY10 head (Boading Longer Precision Pump Co., Ltd., China), over 75 mL of $CaCl_2$ solution under constant stirring. Alginate solutions were dripped with four different needle/tips with internal diameters ranging from 0.25 to 0.50 mm diameter connected to a silicone tube of 1 mm internal diameter, leaving 6.0 (± 0.1) cm between the tip and the gelling bath. Once the last bead was generated, they were maintained in the gelling bath for 5 min. After this period, two protocols were carried out: 1) half of the beads were collected and left in 2 mL of the same calcium chloride solution used as gelling bath (S); 2) the other half was washed out 3 times with distilled water and stored without residual solution (W). A total of 24 bead formulations were prepared (see Fig. S1 in supplementary file). The systems were kept at 4 (± 1) º C until use.

2.3. Beads characterization

Digital image analysis: Area, perimeter, diameter of Feret and roundness were analyzed by performing the “analyze particle” command of the free license software ImageJ as described by Aguirre Calvo and Santagapita (2016). Roundness gives an idea of how far the shape is from sphericity, by relating the area and the major axis of the bead. A digital camera (Canon digital camera, 3.2 Mpix PowerShotA70; Canon Inc., Malaysia; with zoom fixed at 3x) coupled with a binocular microscope (Unitron MS, Unitron Inc., New York, USA, magnification at 7x) was used to take pictures of at least 50 beads for each formulation.

2.4. Microstructural analysis

The structure of the Ca(II)-alginate matrices has been modeled as a mass fractal system of interconnected alginate rods and characterized by small angle X-ray scattering (SAXS) as described in Traffano-Schiffo, Aguirre Calvo, Castro-Giraldez, Fito, and Santagapita, (2017). Three parameters were obtained from the analysis: the rod cross-sectional radius (R), which is obtained from the maximum exhibit by the Kratky plot at $q \approx 1/R$; the fractal dimension at distances higher than R (α_1) describing the multiplicity of the junction zone, and the fractal dimension at distances lower than R (α_2) describing the degree of compactness within the rods. SAXS measurements were performed at the LNLS SAXS2 beamline in Campinas, Brazil, working at $\lambda = 0.1488$ nm and wave vector (q) was selected in the range $0.096\ nm^{-1} < q < 2.856\ nm^{-1}$.

2.5. Water content and activity

Water content (WC) of the beads was determined gravimetrically by difference in weight before and after drying in a vacuum oven for 48 h at 70 (± 2) °C until constant weight. WC was expressed as percentage of grams of water per gram of wet sample (wb). Water activity (a_w) was determined by dew point in a Hygrometer with a special holder to reduce quantity of sample (Aqualab Decagon Devices, Inc., USA). All determinations were made in triplicate.

2.6. Diffusion coefficient

Water diffusion coefficients (D_w) were determined by pulsed magnetic field gradient spin echo (PGSE) sequence in a Low-Field proton Nuclear Magnetic Resonance (LF-^{1}H-NMR) using a Bruker Minispec mq20 spectrometer (Bruker BioSpin GmbH, Rheinstetten, Germany). PGSE consists of a spin echo with the application of two controlled magnetic field gradients applied between 90° and 180° pulses and between 180° pulse and the acquisition (Santagapita et al., 2013). The applied magnetic field gradient intensity was calibrated in the range between 1.4 to 2.5 T m^{-1} ($R^2 = 0.999998$) using a 1.25 g/L $CuSO_4{\cdot}5H_2O$ solution characterized by a known D_w value ($2.30 \pm 0.01{\cdot}10^{-9}$ $m^2\ s^{-1}$ at 25 °C) (Hester-Reilly & Shapley, 2007). Two samples of each bead system were equilibrated at 25 °C in a thermal bath and then setting scans numbers: 16; recycling delay: 2 s; gain: 66 dB; dummy shots: 0; magnetic field amplitude of 1.4 T / m (55% of the total

amplitude), τ (time between the 90° and 180° pulses) of 7.5 ms, δ of 0.5 ms, and Δ of 7.5 ms.

2.7. Mechanical properties of the beads

A compression assay was performed to determine the maximum force that was applied to each of the Ca(II)-alginate beads. A TA-XT2i texture analyzer (Stable Micro Systems, United Kingdom) was employed with a P 0.5 probe (1.27 mm of diameter) by applying a compression of 25% to a single bead, using a test speed of 10 mm/s at room temperature. Calibration of the force (using a 5 kg calibration weight) and the height have been done prior to data collection. Beads were placed centrally, under the probe and the assays were done at least in triplicate.

2.8. Scanning electron microscopy (SEM-FEG)

The morphology of dried beads (at 40 °C for 3 days) was observed by a scanning electron microscopy with field emission gun (SEM-FEG) model supra 40 (Carl Zeiss SMT Inc, Peabody, MA, USA) with InLes detector. Beads were fixed to the SEM's holder using double-sided adhesive tape. Measurements were conducted at 3.00 kV. The sensitivity of the detector allowed to observed beads structure details without applying a metal cover to the samples.

2.9. Statistical analysis

All measurements were analyzed by 2-way ANOVA with Tukey's post-test by using Prism 6.01 (GraphPad Software Inc., San Diego, CA, USA) to assess significant difference between mean values of beads at different synthesis conditions.

3. Results and discussion

3.1. Effect of the synthesis conditions on water status

Water can diffuse through the polymeric matrix altering the volume of the hydrogel leading to bead contraction or expansion. Since water generally travels between gaps in the polymer network, factors altering the space between polymer chains, such as hydrogel charge, composition and density, are expected to have an impact on the water diffusion coefficient (Caccavo, Cascone, Lamberti, & Barba, 2018). The synthesis conditions studied in this work could have an effect on the aforementioned characteristics of the hydrogel, so in order to account for possible implications on water status, it was evaluated by means of water content, activity and diffusion.

Twenty-four bead systems were produced at three pH values, using four extrusion tip sizes and two storage protocols (see Fig. S1 in supplementary file). Fig. 1 shows the water content (WC) for all the synthesized systems. Significant differences were observed for storage protocols (W or S), showing the washed beads (W) higher WC values than those stored in calcium chloride solution (S). This effect is markedly higher for beads synthesized at pH values of 5.0 and 6.8 than for those obtained at pH 3.8. On the other hand, and regardless of the storage protocol employed, the WC is dependent on the extrusion tip size (0.25–0.50 mm). The water content within the bead is related to the process of syneresis throughout the consolidation of the alginate gel network and the diffusion of water molecules through the boundaries of the bead caused by osmotic effects. It is worth noting that both mechanisms of water exchange occur in the surface of the beads, and thus a higher surface to volume ratio (*i. e.* smaller extrusion tip size) is expected to lead to lower values of WC. The differences observed for storage protocols can be explained from the lower ionic content of washed samples (the presence of calcium chloride was observed in the water in equilibrium with W samples, see Fig. S2 in supplementary file), which have implications both in syneresis and osmotic processes.

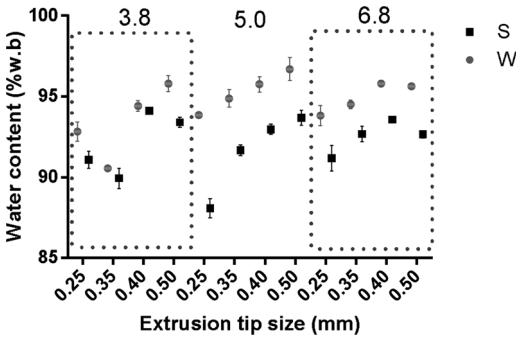

Fig. 1. Water content of Ca(II)-alginate beads systems at pH 3.8, 5.0 and 6.8 for two storage protocols (W and S) and different extrusion tip size. Mean and standard deviation are included.

Table S1 shows measurements accounting for the water availability within the beads: diffusion coefficient and water activity. D_w gives information about the response of water protons modulated by exchange with protons present in the biopolymer chain. Some decrease of the overall mobility of the protons within the matrix is expected for the systems due to the reduced flexibility of the alginate chains in contrast to a water solution. As evidence of this phenomenon, beads exhibited reduced values of D_w ($\sim 2.13 \times 10^{-9}\,m^2 s^{-1}$) compared to the value of pure water ($2.30 \times 10^{-9}\,m^2\,s^{-1}$). High a_w and WC values are obtained as expected and reported (Deladino et al., 2008; Santagapita et al., 2011). When comparing each pair of samples W/S, no significant differences are observed both in D_w and a_w values obtained. Although, taking the entire populations of W and S samples, W samples exhibit higher values of D_w and a_w: $2.14 \pm 0.03 \times 10^{-9}\,m^2\,s^{-1}$ vs. $2.12 \pm 0.03 \times 10^{-9}\,m^2 s^{-1}$ for D_w and 0.989 ± 0.004 vs. 0.986 ± 0.006 for a_w. Then, it is important to highlight that the subtle differences on a_w and D_w obtained by changing extrusion tip size (0.25–0.50), storage protocols (W or S) and synthesis pH (3.8–6.8) are not expected to affect bead performance for industrial applications. These findings suggest that changing the synthesis and storage conditions within the range assessed in the present work does not affect considerably the water availability within the beads.

3.2. Effect of the washing and storage protocol on micro- and macrostructure

The influence of the synthesis conditions on macro and microstructure is shown in Fig. 2, taking the Feret's diameter of beads and the fractal dimension of the alginate rods network (α_1) as representative parameters, respectively. Additional parameters studied (roundness, area and perimeter of beads, and density and size of rods) are shown in Figs. S3 and S4 in Supplementary Information. For samples synthesized at pH 5.0 and 6.8, regardless of the parameter analyzed, there is no significant difference within each pair of samples S and W (related to the washing and storage protocol employed) for any of the synthesis conditions. For samples obtained at more acidic conditions, statistical but very small differences were observed between W/S pairs in those parameters related to the size of the beads, presenting S samples higher values of Area, Perimeter and Feret's diameter. Concerning microstructural parameters, no significant differences were observed varying the washing and storage protocol of samples.

The performance of these systems in terms of mechanical properties of the beads is expected to be highly related to some of these micro- and macroscopic parameters. Mechanical strength should be examined when considering potential food and medical applications of Ca(II)-alginate beads as encapsulation agents since it indicates the susceptibility of the beads to different environments, transportation in fluids and exposure to shear forces (Bhujbal, Paredes-Juarez, Niclou, & de Vos, 2014). The required force to compress the beads to a 25% of their size is

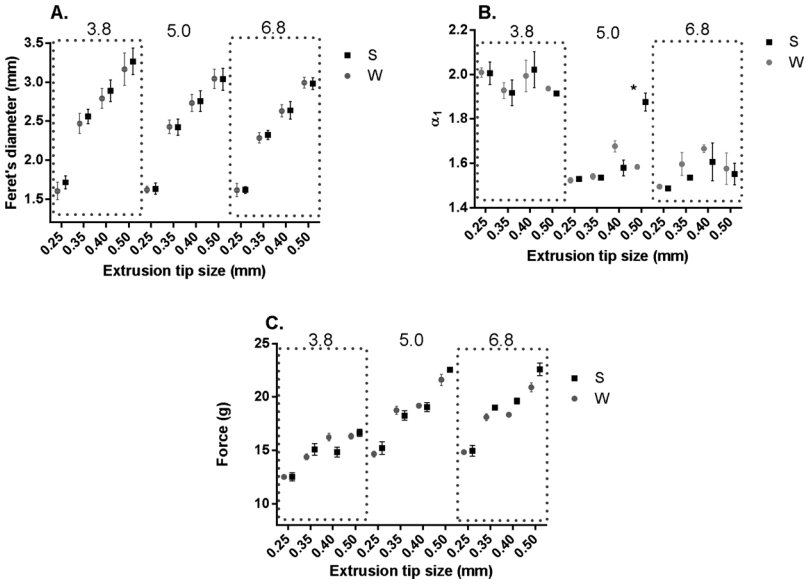

Fig. 2. A) Feret's diameter by image analysis, **B)** interconnectivity of rods by SAXS (α_1) and C**)** mechanical strength by texture analyzer obtained for Ca(II)-alginate beads systems at pH 3.8, 5.0 and 6.8 for two storage protocols (W and S) and different extrusion tip size. Mean and standard deviation are included. The * corresponds to an outlier.

shown in Fig. 2C. As a general trend, no significant differences between storage protocols were found in the strength of beads (Fig. 2C), even though some small differences were observed for the samples synthesized at pH 6.8. Thus, these results indicate that with these synthesis and storage conditions, 5 min are enough for consolidation of the alginate network.

In view of these results, the step of washing the alginate beads to remove residual Ca^{2+} ions and the storage conditions have no implications in the structure of the alginate network nor in the macroscopic properties of beads. These findings are crucial for technological applications, allowing the reduction of time and costs. It should be noted that altering the M/G composition of sodium alginate, synthesis concentrations of alginate and calcium chloride and the solutions used as storage medium may have some impact on the development of the crosslinked structure and mechanical properties of the beads over time and during storage (Bhujbal, Paredes-Juarez et al., 2014, 2014).

3.3. Effect of the extrusion tip size

Fig. 3 shows the influence of the extrusion tip size on Feret's diameter, roundness, area and perimeter of beads evaluated by combining W and S data for each system. As expected, the Feret's diameter, area, perimeter of the obtained beads show an increase with the increment of the internal diameter of the extrusion tip/needle size in agreement with previously reported results (Aguirre Calvo et al., 2017; Aguirre-Calvo et al., 2018; Deladino et al., 2008; Ramos et al., 2018). Besides, roundness is influenced by the synthesis pH (as will be further discussed) and does not show dependence with the extrusion tip size.

It is worth noting that, within the conditions of synthesis evaluated in this study, the mean values of microstructural parameters were not influenced by the size of the alginate bead (as already shown in Fig. 2A). Even though it has been demonstrated that the crosslinking cation concentration gradient within the forming bead during the ionotropic gelation process results in inhomogeneities of the alginate microstructure (Sonego et al., 2016), these differences were not manifested under current evaluation. Besides, differences in the diffusion and availability of the crosslinking cation that can be modulated by the surface-to-volume ratio (and hence the size of the initial drop, determined by the extrusion tip size) can also be considered negligible at this observational scale.

On the other hand, the mechanical strength results presented in Fig. 2C showed that the strength required for compression increased as the size of the beads increases, in accordance to Bhujbal, Paredes-Juarez et al. (2014) findings. For the same pH, bigger beads can accommodate more divalent ions in their core which lead to more crosslinked structures increasing the global mechanical stability of the beads. pH also plays a role, as will be further discussed in next sections.

3.4. Effect of the synthesis pH on microstructural parameters

Tuning the microstructure of the alginate matrix is a stepping stone toward the rational design of these systems, since it determines the macroscopic porosity, the loading efficiency of encapsulated compounds and their release behavior, among other relevant parameters (Perullini, Jobbágy, Soler-Illia, & Bilmes, 2005). In this scenario, understanding how the microstructure is affected within the typical range of working pH for labile compounds encapsulation is of prime importance for the optimization of technological applications.

It is well established that the microstructure of the alginate networks obtained at acidic conditions (below pH 3.5) significantly differ from those obtained by conventional ionotropic gelation. In particular, in a recent work we showed that H-alginate presented a 3-fold increase in the value of parameter α_1 (degree of interconnection of the rods composing the structure) and a 50% increase in parameter R (the rod cross-sectional radius) with respect to a conventional Ca(II)-alginate network synthesized at neutral pH. Moreover, we demonstrated that the Ca(II) sample obtained by cation exchange from the H–alginate hydrogel maintains the structural pattern from the parent hydrogel (Sonego et al., 2016).

Here we analyze the impact of driving an ionotropic gelation at acidic conditions on the microstructure of the hydrogel, in order to evaluate if there is a contribution from the expected higher alginate chain-chain interactions. The working pH values were chosen to include: the more extended pH of work which corresponds to a pure sodium alginate solution (6.8), and an acidic value of pH without reaching the point of gelation (3.8).

Fig. 4 shows the influence of pH on the microstructural parameters of the beads. For each pH, every system (different storage protocols and extrusion tip sizes) is represented in the graph. Statistical analysis suggests that the effects caused by the storage protocol and the extrusion tip size on the consolidation of the alginate network are negligible which is evidenced by the low dispersion observed in each group. Thus, microstructural parameters in our systems are only influenced by the pH of synthesis. Samples obtained at pH 3.8 showed the highest values of all the parameters analyzed, while no significant differences were found between the group of samples obtained at pH 5.0 and 6.8.

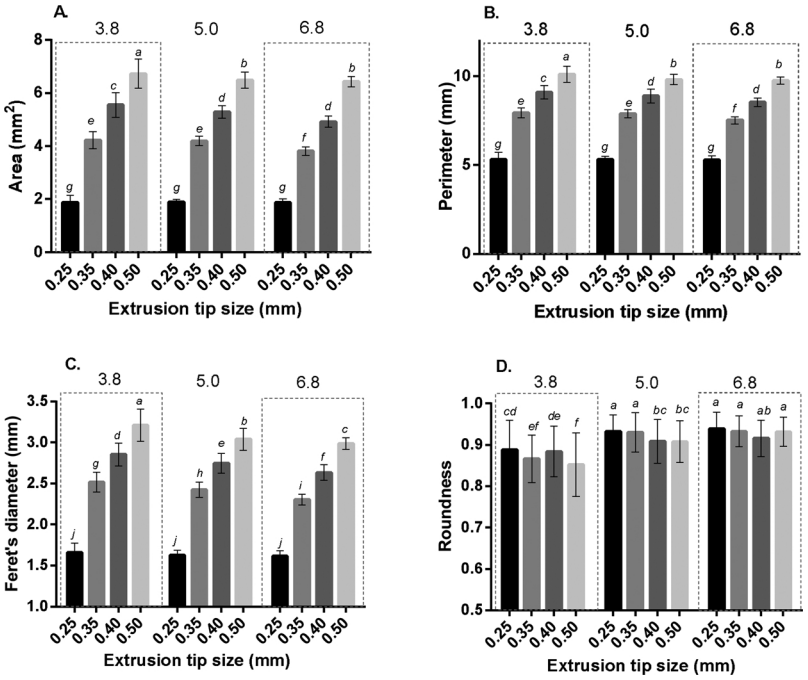

Fig. 3. Influence of the extrusion tip size (samples arranged increasing needle/tip extrusion diameter: 0.25 mm, 0.35 mm, 0.40 mm, and 0.50 mm, respectively) on **A.** Area, **B.** Perimeter, **C.** Feret's diameter and **D.** Roundness of Ca(II)-alginate beads systems obtained at pH 3.8, 5.0 and 6.8. Mean and standard deviation are included. Different lower-case letters on columns indicate significant differences among means comparing all samples (among extrusion tip and pH).

Likewise, the pH of synthesis affects the mechanical properties of the beads. Beads synthesized at pH 5.0 and 6.8 show a similar trend in the force required for compression (Fig. 2C), while those synthetized at pH 3.8 require considerably less force to obtain the same compression indicating less strength. The uronic acid residues, which constitute the alginate polymer, create junction zones within the gel. As the gelation process occurs, junction zones build up until saturation of the gel is obtained. When more cations participate in this process, larger and more junction zones are generated which increases the chance of uncoupling occurring in the junction zone. When junction zones break, acceleration of the uncoupling of neighboring chains occurs. Bhujbal, Paredes-Juarez et al. (2014) found that beads obtained with shorter times of gelation exhibited more strength than those obtained with longer gelling time attributing these results to the degree of saturation of the gel, thus, the amount of junction zones within it. In a similar way, working at acidic conditions may lead to the formation of more junction zones, since alginate chains are more compact and interconnected, as demonstrated by higher values of α_2 and α_1 obtained by SAXS (Fig. 4), leading to an increased formation of junction zones, and hence accelerating the uncoupling occurring in the junctions and weakening the structure when subjected to compression.

3.5. Model of chain-chain interactions and polymer chain packing

Fig. 5 schematically represents the time course of the gelation process. The working pH value of 3.8 is above the pKa of the alginate

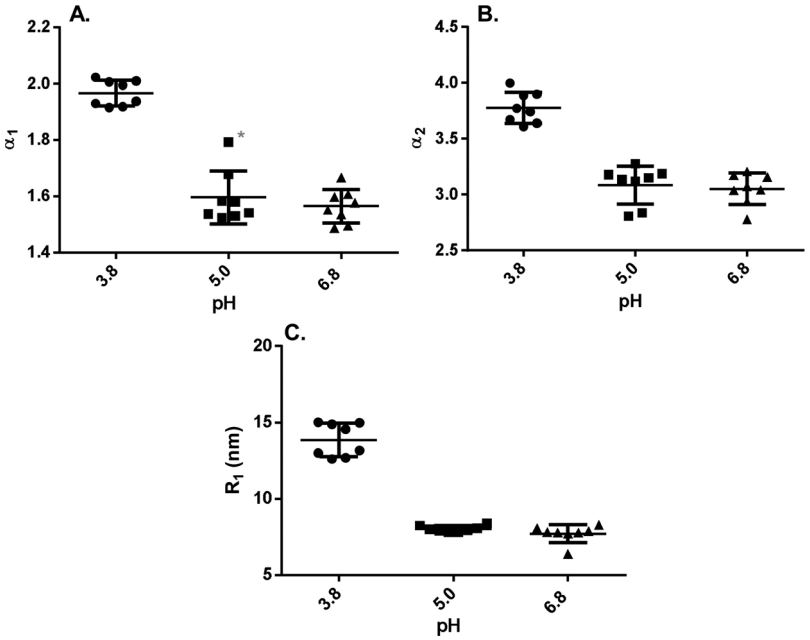

Fig. 4. Influence of the synthesis pH (3.8, 5.0 and 6.8) on the microstructural parameters of Ca(II)-alginate hydrogels: **A)** interconnectivity (α_1), **B)** density (α_2) and **C)** size (R) of the alginate rods. Mean and standard deviation are included. The * corresponds to an outlier.

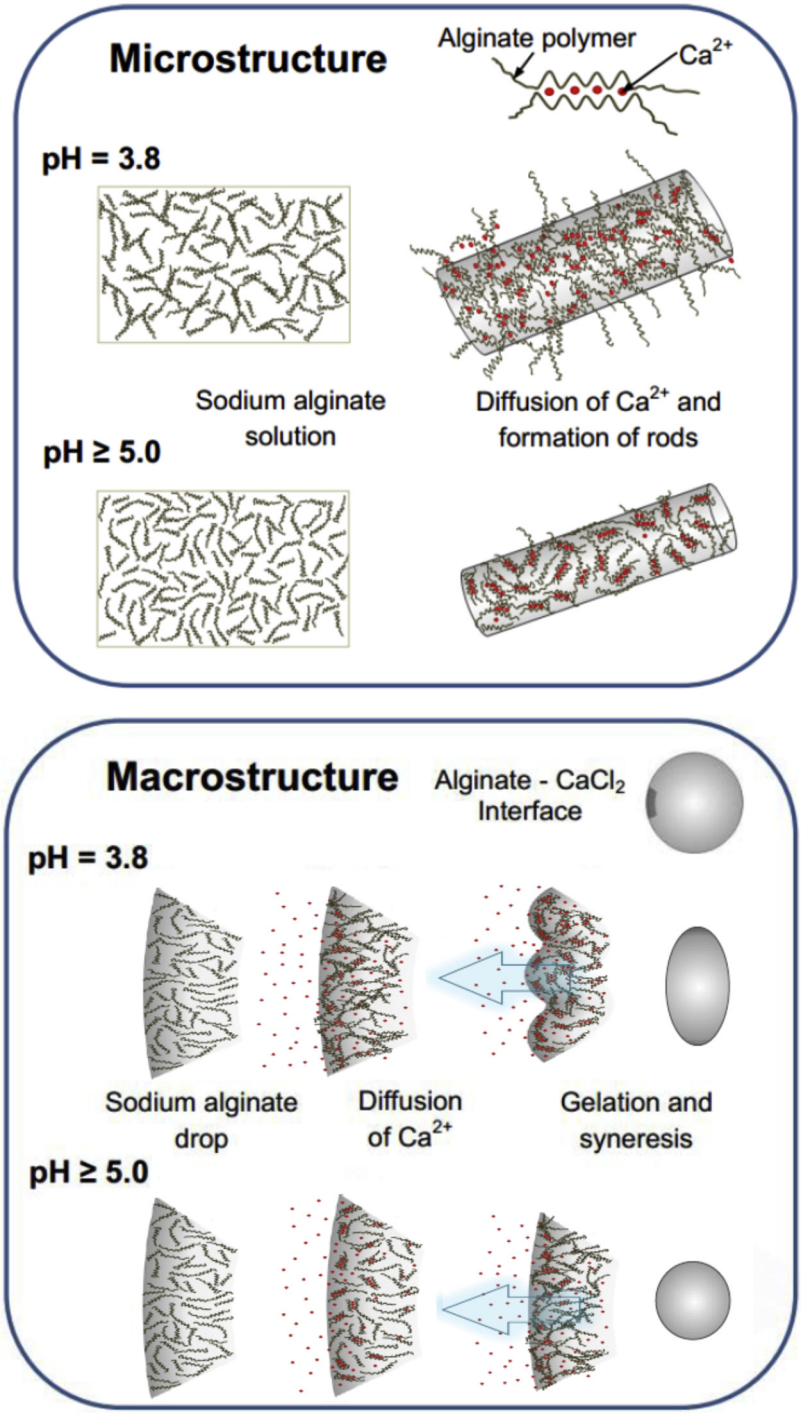

Fig. 5. Schematic representation of the gelation process for samples synthesized at pH 3.8 and at pH values far from the pKa of the alginate polymer residues (samples synthesized at pH 5.0 and 6.8), showing details at the micro- and macroscopic scales. For samples synthesized at pH 3.8, the stronger chain-chain interactions of partially protonated alginate polymers generate supramolecular branched blocks of construction leading to a more structured network in the front of gelation. This effect explains both, a hindered syneresis and shrinkage of the system. By the contrary, multiple events of rearrangement in the Ca(II)-alginate/solution interface are allowed in the samples synthesized at near neutral pH conditions, leading to syneresis and shrinkage of the bead, maintaining its spherical macroscopic conformation.

polymer residues (3.38 and 3.65 for M and G, respectively). In these conditions, enhanced chain-chain interactions generate supramolecular structures that, without reaching percolation, constitute branched pre-structures on which ionotropic gelation occurs. Thus, with the addition of Ca^{2+} cations, the lower electrostatic repulsion determines a denser packing of polymer chains within the alginate rods as well as a higher middle size of these rods (higher values of parameters α_2 and R, respectively) compared to the samples synthesized at higher pH values (5.0 and 6.8) (see Fig. 4B and C). Additionally, from the more branched blocks of construction preformed at the acidic condition, the resulting network is expected to be more ramified (higher value of parameter α_1) compared to that obtained at near neutral pH conditions (see Fig. 4A).

From a macroscopic point of view, starting from larger and more branched blocks of construction causes the network to consolidate more quickly. As depicted in Fig. 5, this is expected to have a huge effect on the promptness of rearrangement of this incipient network in the boundaries of alginate-$CaCl_2$ solution interface. As a general trend, those samples synthesized at pH 3.8 present a higher bead size (reflected in a higher area, perimeter and Feret´s diameter; see Fig. 3A–C) and a lower roundness (see Fig. 3D). Both tendencies are explained by the hindered rearrangement of a more consolidated and branched network in the front of gelation of the beads. Besides, the differences in water content for systems obtained at pH 3.8, can be explained from the impeded syneresis in higher structured alginate network.

Surface morphology of beads obtained by SEM images (Fig. 6) confirms that the main differences are attributable to the pH of

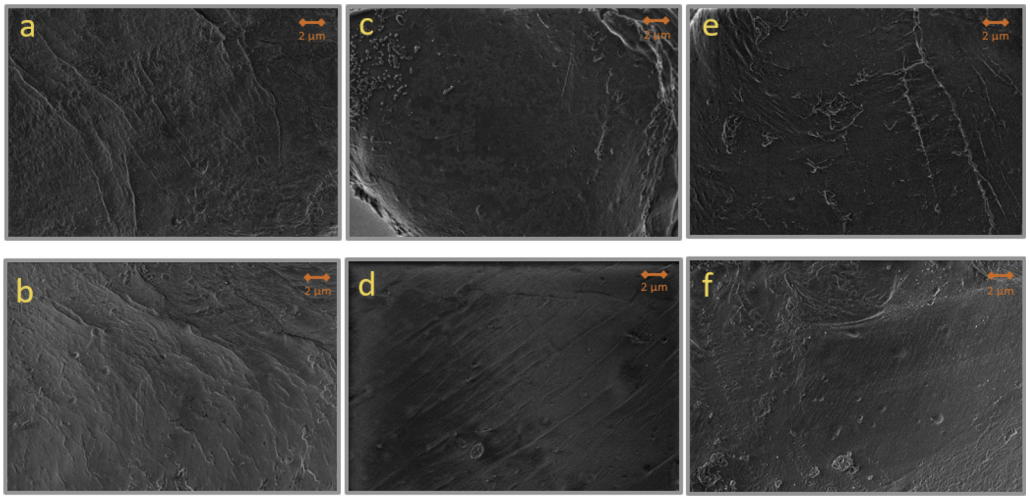

Fig. 6. Scanning electron microscopic images of surface morphology of Ca(II)-alginate beads synthetized at pH 3.8 (a & b), pH 5.0 (c & d) and at pH 6.8 (e & f) for two storage protocols (W and S), respectively. A 0.50 mm extrusion tip size was used in all cases.

synthesis. The surface of the beads obtained at pH 3.8, regardless of storage protocol employed, shows wrinkles and cavities and in general less homogeneity than the surface of those obtained at pH 5.0 and 6.8, which appear to be smoother. This is well in line with the hypothesis of impeded rearrangement of a more consolidated network at pH 3.8. SEM images corroborate that storage protocols (W and S) do not have a major impact on the alginate network and consolidation of the beads.

4. Conclusions

The results obtained in the present work allow to scale and standardize the process of alginate beads production at an industrial level by managing three synthesis variables: pH, extrusion tip size and washing and storage protocol. Several practical implications can be remarked: in the first place, the washing and storage protocol does not have a major influence on micro- and macroscopic parameters of beads. Ruling out this procedure could save time and cost by reducing waste management. The performance of these systems (for instance in terms of mechanical properties and stability of the beads in operating conditions) is expected to be highly related to these micro- and macroscopic parameters. However, these properties should be further analyzed when critical for a certain application. In the second place, the extrusion tip size is not relevant for the consolidation of the microstructure, water availability and mobility, but will influence the water content, size of the beads and mechanical strength. In the third place, the pH of synthesis causes changes at microstructural level (alginate rod size, density and interconnectivity) as well as macrostructural level (bead area, roundness and mechanical strength) and in the morphology of the surface.

We present a model in which the stronger chain-chain interactions of partially protonated alginate polymers (working above but close to the pKa of the alginate residues), generate supramolecular branched blocks of construction leading to different special arrangements in the front of gelation. In turn, the different nature of these incipient networks (obtained at acidic or near neutral pH), determine micro- and macroscopic changes in structural parameters of the obtained systems.

Different alginate and calcium concentrations, alginate M/G ratios and gelation times will be analyzed in future works for a deeper and univocal description of the behavior of this relevant system. Tuning the structure of the alginate matrix is expected to affect relevant parameters such as sorption, exchange and transport kinetics, as well as the mechanical properties and the stability of the obtained hydrogels in working conditions. These physicochemical parameters define the performance of these systems in most of the present and potential biomedical and environmental applications.

Acknowledgments

This work was supported by the Brazilian Synchrotron Light Laboratory (LNLS, Brazil, proposal 20170187), Agencia Nacional de Promoción Científica y Tecnológica (ANPCyT PICT 2014 2582) and CIN-CONICET (PDTS 2015-196). MP and PRS are Research Scientists of CONICET (Argentina).

Appendix A. Supplementary data

Supplementary material related to this article can be found, in the online version, at doi:https://doi.org/10.1016/j.carbpol.2018.11.051.

References

Aguirre Calvo, T. R., & Santagapita, P. R. (2016). Physicochemical characterization of alginate beads containing sugars and biopolymers. *Journal of Quality and Reliability Engineering* ID:9184039.

Aguirre Calvo, T. R., Busch, V. M., & Santagapita, P. R. (2017). Stability and release of an encapsulated solvent-free lycopene extract in alginate-based beads. *LWT - Food Science and Technology, 77*, 406–412.

Aguirre-Calvo, T. R., Perullini, A. M., & Santagapita, P. R. (2018). Encapsulation of betacyanins and polyphenols extracted from leaves and stems of beetroot in Ca(II)-alginate beads: A structural study. *Journal of Food Engineering, 235*, 32–40.

Agulhon, P., Robitzer, M., David, L., & Quignard, F. (2012). Structural regime identification in ionotropic alginate gels: Influence of the cation nature and alginate structure. *Biomacromolecules, 13*(1), 215–220.

Bhujbal, S. V., Paredes-Juarez, G. A., Niclou, S. P., & de Vos, P. (2014). Factors influencing the mechanical stability of alginate beads applicable for immunoisolation of mammalian cells. *Journal of the Mechanical Behavior of Biomedical Materials, 37*, 196–208.

Bhujbal, S. V., de Vos, P., & Niclou, S. P. (2014). Drug and cell encapsulation: Alternative delivery options for the treatment of malignant brain tumors. *Advanced Drug Delivery Reviews, 67–68*, 142–215.

Biswas, S., Chattopadhyy, M., Sen, K. K., & Saha, M. K. (2015). Development and characterization of alginate coated low molecular weight chitosan nanoparticles as new carriers for oral vaccine delivery in mice. *Carbohydrate Polymers, 121*, 403–410.

Caccavo, D., Cascone, S., Lamberti, G., & Barba, A. A. (2018). Hydrogels: Experimental characterization and mathematical modelling of their mechanical and diffusive behavior. *Chemical Society Reviews, 47*(7), 2357–2373.

Deladino, L., Anbinder, P. S., Navarro, A. S., & Martino, M. N. (2008). Encapsulation of natural antioxidants extracted from *Ilex paraguariensis*. *Carbohydrate Polymers, 71*(1), 126–134.

Draget, K. I., & Taylor, C. (2011). Chemical, physical and biological properties of alginates and their biomedical implications. *Food Hydrocolloids, 25*(2), 251–256.

He, X., Liu, Y., Li, H., & Li, H. (2016). Single-stranded structure of alginate and its conformation evolvement after an interaction with calcium ions as revealed by electron microscopy. *RSC Advances, 6*(115), 114779–114782.

Hester-Reilly, H. J., & Shapley, N. C. (2007). Imaging contrast effects in alginate microbeads containing trapped emulsion droplets. *Journal of Magnetic Resonance,*

188(1), 168–175.
Hoare, T. R., & Kohane, D. S. (2008). Hydrogels in drug delivery: Progress and challenges. *Polymer, 49*, 1993–2007.
Lee, K. Y., & Mooney, D. J. (2012). Alginate: Properties and biomedical applications. *Progress in Polymer Science, 37*, 106–126. https://doi.org/10.1016/j.progpolymsci.2011.06.003.
Li, Y., Feng, C., Li, J., Mu, Y., Liu, Y., Kong, M., et al. (2017). Construction of multilayer alginate hydrogel beads for oral delivery of probiotics cells. *International Journal of Biological Macromolecules, 105*, 924–930.
Narayanan, R. P., Melman, G., Letourneau, N. J., Mendelson, N. L., & Melman, A. (2012). Photodegradable iron (III) cross-linked alginate gels. *Biomacromolecules, 13*, 2465–2471.
Nedovic, V., Kalusevic, A., Manojlovic, V., Levic, S., & Bugarski, B. (2011). An overview of encapsulation technologies for food applications. *Procedia Food Science, 1*, 1806–1815.
Perullini, M., Jobbágy, M., Soler-Illia, G. J. A. A., & Bilmes, S. A. (2005). Cell growth at cavities created inside silica monoliths synthesized by sol-gel. *Chemistry of Materials, 17*(15), 3806–3808.
Perullini, M., Orias, F., Durrieu, C., Jobbágy, M., & Bilmes, S. A. (2014). Co-encapsulation of *Daphnia magna* and microalgae in silica matrices, a stepping stone toward a portable microcosm. *Biotechnology Reports, 4*, 147–150.
Ramos, P. E., Silva, P., Alario, M. M., Pastrana, L. M., Teixeira, J. A., Cerqueira, M. A., et al. (2018). Effect of alginate molecular weight and M/G ratio in beads properties foreseeing the protection of probiotics. *Food Hydrocolloids, 77*, 8–16.
Rowley, J. A., Madlambayan, G., & Mooney, D. J. (1999). Alginate hydrogels as synthetic extracellular matrix materials. *Biomaterials, 20*, 45–53.
Santagapita, P. R., Mazzobre, M. F., & Buera, M. P. (2011). Formulation and drying of alginate beads for controlled release and stabilization of invertase. *Biomacromolecules, 12*(9), 3147–3155.
Santagapita, P. R., Laghi, L., Panarese, V., Tylewicz, U., Rocculi, P., & Dalla Rosa, M. (2013). Modification of transverse NMR relaxation times and water diffusion coefficients of kiwifruit pericarp tissue subjected to osmotic dehydration. *Food and Bioprocess Technology, 6*, 1434–1443.
Sarkar, N., Sahoo, G., Das, R., Prusty, G., & Swain, S. K. (2017). Carbon quantum dot tailored calcium alginate hydrogel for pH responsive controlled delivery of vancomycin. *European Journal of Pharmaceutical Sciences: Official Journal of the European Federation for Pharmaceutical Sciences, 109*, 359–371.
Sonego, J. M., Santagapita, P. R., Perullini, M., & Jobbágy, M. (2016). Ca(II) and Ce(III) homogeneous alginate hydrogels from the parent alginic acid precursor: A structural study. *Dalton Transactions, 45*(24), 10050–10057.
Spedalieri, C., Sicard, C., Perullini, M., Brayner, R., Coradin, T., Livage, J., et al. (2015). Silica@proton-alginate microreactors: A versatile platform for cell encapsulation. *Journal of Materials Chemistry, 3*, 3189–3194.
Stokke, B. T., Draget, K. I., Smidsrod, O., Yuguchi, Y., Urakawa, H., & Kajiwara, K. (2000). Small-angle X-ray scattering and rheological characterization of alginate gels. 1. Ca-alginate gels. *Macromolecules, 33*(5), 1853–1863.
Traffano-Schiffo, M. V., Aguirre Calvo, T. R., Castro-Giraldez, M., Fito, P. J., & Santagapita, P. R. (2017). Alginate beads containing lactase: Stability and microstructure. *Biomacromolecules, 18*, 1785–1792.
Traffano-Schiffo, M. V., Castro-Giraldez, M., Fito, P. J., Perullini, M., & Santagapita, P. R. (2018). Gums induced microstructure stability in Ca(II)-alginate beads containing lactase analyzed by SAXS. *Carbohydrate Polymers, 179*, 402–407.
Wandrey, C., Bartkowiak, A., & Harding, S. E. (2009). Materials for encapsulation. In N. J. Zuidam, & V. A. Nedovic (Eds.). *Encapsulation technologies for food active ingredients and food processing* (pp. 31–100). Dordrecht, The Netherlands: Springer.